Anteriorization of neural fate by inhibitor of β-catenin and T cell factor (ICAT), a negative regulator of Wnt signaling

Kiyotoshi Satoh*, Mana Kasai*, Takefumi Ishidao*, Kenichi Tago*†, Susumu Ohwada†, Yoshimi Hasegawa‡, Takao Senda‡, Shinji Takada§, Shigeyuki Nada¶, Tsutomu Nakamura*, and Tetsu Akiyama*‖

*Laboratory of Molecular and Genetic Information, Institute for Molecular and Cellular Biosciences, University of Tokyo, 1-1-1 Yayoi, Bunkyo-ku, Tokyo 113-0032, Japan; †Department of Surgery, Gunma University Graduate School of Medicine, 3-39-22 Showa-machi, Maebashi, Gunma 371-8511, Japan; ‡Department of Anatomy I, Fujita Health University School of Medicine, Aichi 470-1192, Japan; §Center for Molecular and Developmental Biology, Graduate School of Science, Kyoto University, Kitashirakawa, Sakyo-ku, Kyoto 606-8502, Japan; and ¶Department of Oncogene Research, Research Institute for Microbial Disease, Osaka University, 3-1 Yamadaoka, Suita, Osaka 565-0871, Japan

Edited by John C. Gerhart, University of California, Berkeley, CA, and approved April 12, 2004 (received for review March 11, 2004)

Inhibitor of β-catenin and T cell factor (ICAT) inhibits Wnt signaling by interfering with the interaction between β-catenin and T cell factor. Here we show that ICAT$^{-/-}$ embryos exhibit malformation of the forebrain and craniofacial bones and lack the kidney. Analysis of the neuronal differentiation of embryonic stem cells revealed that Wnt3a redirects the fate of neural progenitors to a posterior character, whereas ICAT induces forebrain cells by inhibiting Wnt signaling. Furthermore, ICAT$^{-/-}$ embryonic stem cells were found to differentiate into neuronal cells possessing a posterior character. These results suggest that ICAT plays an important role in the anteriorization of neural cells by inhibiting the posteriorizing activity of Wnt signaling.

Wnt signaling plays a crucial role in a number of developmental processes, including body axis formation, development of the central nervous system, and axial specification in limb development (1–8). Wnt signaling stabilizes β-catenin, which in turn associates with T cell factor (TCF)/lymphoid-enhancing factor family transcription factors, ultimately altering the expression of Wnt target genes. In the absence of Wnt signaling, β-catenin is recruited into the multiprotein complex containing adenomatous polyposis coli (APC), glycogen synthase kinase-3β, casein kinase 1α, and Axin or the closely related factor conductin/Axil and subjected to proteasome-mediated degradation. Wnt signaling is further inhibited by the association of β-catenin with the inhibitor of β-catenin and TCF (ICAT) (9–12). ICAT is an 81-aa protein that interferes with the interaction between β-catenin and TCF. ICAT contains an amino-terminal helical domain that binds to armadillo repeats 10–12 of β-catenin, and a carboxy-terminal tail that competes with TCF for binding to armadillo repeats 5–10 (9, 11, 12). Overexpression of ICAT induces G_2 arrest and cell death of colorectal tumor cells mutated in APC or β-catenin and hepatocellular carcinoma cells mutated in Axin (10).

It has been shown that Wnt signaling specifies posterior-to-anterior fates within the neural plate (13–16). Inhibition of Wnt signaling is required for anterior specification; negative regulators of Wnt signaling play a crucial role in establishing a gradient of Wnt activity patterning the anterior–posterior axis. Mouse embryos lacking Dickkopf1, a secreted protein that acts as an inhibitor of the Wnt coreceptor low density lipoprotein receptor-related protein 6, lack head structures anterior to the midbrain (17). Also, mouse embryos lacking Six3 (sine oculis homeobox homolog 3), a direct negative regulator of Wnt1 expression, lack forebrain structures and exhibit posteriorization of the remaining mutant heads (18). In addition, zebrafish mutants for the negative intracellular regulators of Wnt signaling *tcf3/headless* and *axin/masterblind* display anterior defects (19–21). In the present study, we show that mouse embryos lacking ICAT exhibit multiple defects including malformation of the forebrain. Furthermore, by analyzing the neuronal differentiation of embryonic stem (ES) cells, we demonstrate that ICAT induces forebrain cells by inhibiting Wnt signaling.

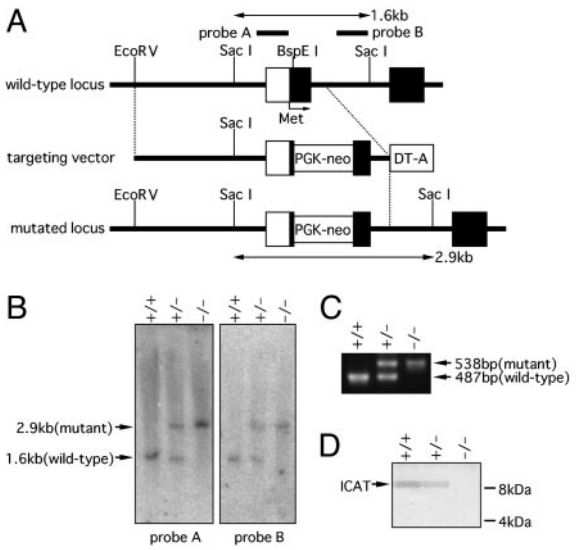

Fig. 1. Targeted disruption of ICAT. (*A*) ICAT was inactivated by the insertion of a neomycin resistance cassette (PGK-neo) in the *Bsp*EI site located 11 aa downstream of the first initiation methionine (Met). Open and filled boxes represent noncoding and coding exons, respectively. The diphtheria toxin A cassette (DT-A) was placed outside the 3′ homologous region for negative selection. (*B*) The mutated ICAT locus was identified by Southern blot analysis of genomic DNA digested with *Sac*I and hybridized to internal (probe A) and external (probe B) genomic fragments. The 1.6-kb fragment represents the wild-type allele, and the 2.9-kb fragment represents the mutated allele. (*C*) PCR analysis of mutant mice. ICAT primers 1 and 2 were used to amplify the wild-type allele; neo primer and ICAT primer 1 were used to amplify the mutant allele. (*D*) Immunoblot analysis of mutant mice. Lysates prepared from embryos were subjected to immunoprecipitation with anti-ICAT antibody, fractionated by SDS/PAGE, and immunoblotted with anti-ICAT antibody.

Materials and Methods

Functional Inactivation of ICAT. The targeting vector was constructed by inserting a neomycin resistance cassette into the

This paper was submitted directly (Track II) to the PNAS office.

Abbreviations: ES, embryonic stem; TCF, T cell factor; ICAT, inhibitor of β-catenin and TCF; BF-1, brain factor 1; E*n*, embryonic day *n*; SDIA, stromal cell-derived inducing activity.

‖To whom correspondence should be addressed. E-mail: akiyama@iam.u-tokyo.ac.jp.

Fig. 2. Inactivation of ICAT results in multiple developmental defects. (*A–C*) Wild-type [*A* (left) and *B*] and ICAT$^{-/-}$ [*A* (right) and *C*] embryos at E18.5 are shown. Some ICAT$^{-/-}$ embryos exhibited exencephaly and lacked eyes, nose, maxillary bone, and rostral skull. The tongue (arrowhead) and stunted brain (red arrow) were exposed and head skin was turned outside (white arrow). ICAT$^{-/-}$ embryos were slightly pale. (*D*) In E12.5 ICAT$^{-/-}$ embryos (right), the rostral head is truncated (arrow). (*E*) The brains of embryos at E18.5 were fixed in Bouin's reagent. Development of the cerebrum in ICAT$^{-/-}$ embryos was defective (arrowhead). (*F*) The upper jaws of embryos at E18.5 were fixed in Bouin's reagent. ICAT$^{-/-}$ (right) embryos had a cleft secondary palate (arrow). (*G* and *H*) Terminal deoxynucleotidyltransferase-mediated dUTP nick end labeling (TUNEL) stains of the sections of the first branchial arch from wild-type (*G*) and ICAT$^{-/-}$ (*H*) embryos at E11.0 are shown. ICAT$^{-/-}$ embryos had an increased number of apoptotic cells (arrow). (*I*) In ICAT$^{-/-}$ (right) mice, the gut expanded and ruptured immediately after birth. (*J* and *K*) The urogenital systems of wild-type (*J*) and ICAT$^{-/-}$ (*K*) embryos at E18.5 are shown. In ICAT$^{-/-}$ embryos, the adrenal glands (arrowhead) were present but kidneys were absent. The arrows in *J* point to the kidneys.

*Bsp*EI site located 11 aa downstream of the first initiation methionine, preserving 7.2 kb (5′) and 0.42 kb (3′) of the flanking homologous regions. TT2 ES cells were electroporated and selected by following standard procedures. Surviving clones were screened for homologous recombination by PCR with the following primers: neo primer (5-TCGTGCTTTACGGTATCGCCGCTCCCGATT-3′), which is homologous to the neomycin resistance gene, and ICAT primer 1 (5′-TCTGGCGCAGGGCAGGTAGGAACGTTCAGG-3′), which lies just downstream of the 3′ homologous region in the targeting vector; the wild-type allele was amplified by PCR with ICAT primers 1 and 2 (5′-TGAACCGCGAGGGAGCACCCGGGAAGAGTC-3′), which lie just upstream of the *Bsp*EI site. Correctly targeted clones were used for aggregation with eight-cell embryos, and chimeric males were mated with C57BL/6 females.

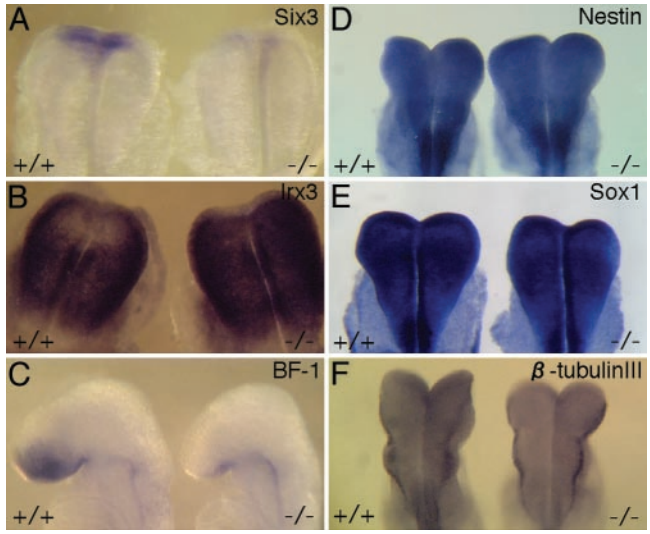

Fig. 3. ICAT$^{-/-}$ embryos lack the anterior neural plate. Whole-mount *in situ* hybridization of E8.0–E8.5 embryos was performed. (*A*) The anterior neural plate marker Six3 was barely detectable in ICAT$^{-/-}$ (right) embryos at E8.0 (1- to 2-somites stage). (*B*) In E8.0 wild-type embryos (left), Irx3 was expressed in the posterior neural plate, complementarily to Six3 expression in the anterior plate. In ICAT$^{-/-}$ (right) embryos, Irx3 was also expressed in the anterior neural plate (1- to 2-somites stage). (*C*) The anterior neural plate expressing BF-1 was barely detectable in ICAT$^{-/-}$ (right) embryos at E8.5 (8- to 10-somites stage). (*D*) The neural progenitor marker Nestin was similarly expressed in wild-type (left) and ICAT$^{-/-}$ (right) embryos at E8.5 (5- to 6-somites stage). (*E*) Neural progenitor cells expressing Sox1 were normally induced in ICAT$^{-/-}$ embryos at E8.5 (right) (5- to 6-somites stage). (*F*) Expression of class III β-tubulin, a marker for differentiating neurons, at E8.5 appears normal in ICAT$^{-/-}$ embryos (right) (7- to 9-somites stage).

Embryo Histology and *in Situ* Hybridization Analysis. Embryos were fixed in 4% paraformaldehyde and processed for whole-mount *in situ* hybridization by following standard procedures. Single-stranded RNA probes were labeled with digoxigenin-UTP according to the manufacturer's instructions (Roche).

Neural Induction from ES Cells. For differentiation, ES cells were cultured on PA6 cells to form colonies from a single cell (22). PA6 cells were plated on collagen-coated slides or gelatin-coated dishes and fixed in 4% paraformaldehyde before coculturing with ES cells. The day on which ES cells were seeded on PA6 was designated day 0. Soluble Wnt3a and control-conditioned media were obtained from L cells transfected with *Wnt3a* (23). The coding region of ICAT was inserted into the pCAG-IP vector, which enables episomal expression in MG1.19 ES cells (24). ES cells were transfected by Lipofectamine 2000 (Invitrogen) by following the manufacturer's instructions. Because pCAG-IP encodes a puromycin resistance gene, transfected cells were selected in the presence of 1 μg/ml puromycin.

RNA Extraction and Semiquantitative RT-PCR Analysis. Total cellular RNA was prepared by using NucleoSpin RNA II (Macherey & Nagel). For cDNA synthesis, random hexamer primers were used to prime reverse transcriptase reactions. cDNA synthesis was carried out by using Moloney murine leukemia virus Superscript III reverse transcriptase (Invitrogen) following the manufacturer's instructions. Cycling parameters for PCR were as follows: denaturation at 94°C for 20 sec; annealing at 60–70°C for 20 sec, depending on the primer; and elongation at 72°C for 2 min. The number of cycles varied between 25 and 35, depending on the respective mRNA abundance.

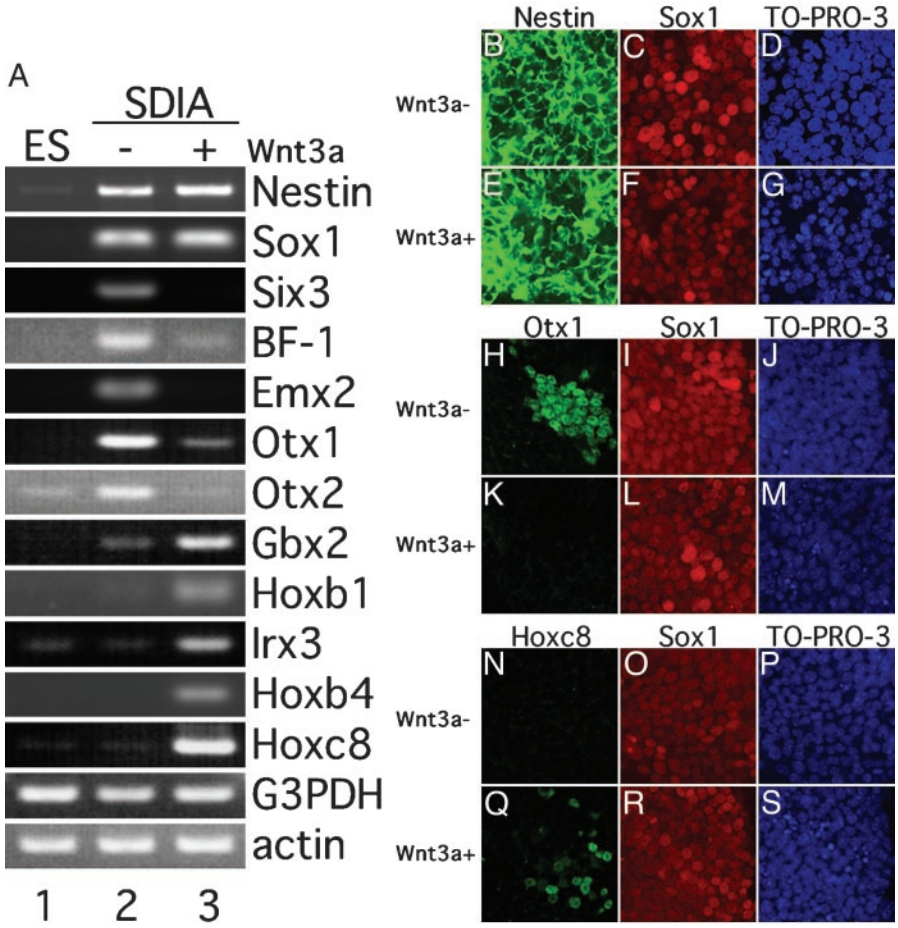

Fig. 4. Wnt signaling changes the fate of neural progenitors that differentiated from ES cells into a posterior character. (*A*) Semiquantitative RT-PCR analysis of Wnt3a-treated ES cells. Lane 1, undifferentiated ES cells. Lanes 2 and 3, SDIA-treated ES cells without or with Wnt3a treatment during days 2–6. Total RNA was isolated on day 6. Wnt3a treatment suppressed the forebrain markers Six3, BF-1, Emx2, Otx1, and Otx2 and induced the hindbrain markers Gbx2 and Hoxb1 and the spinal cord markers Irx3, Hoxb4, and Hoxc8. The levels of Nestin and Sox1 expression were not significantly affected. (*B–S*) Double immunostaining of SDIA-treated ES cells without (*B–D*, *H–J*, and *N–P*) or with (*E–G*, *K–M*, and *Q–S*) Wnt3a treatment during days 2–6. The day on which ES cells were seeded on PA6 was designated day 0. (*B–G*) Cells were double-stained with anti-Nestin and anti-Sox1 antibodies. (*H–M*) Cells were double-stained with anti-Otx1 and anti-Sox1 antibodies. (*N–S*) Cells were double-stained with anti-Hoxc8 and anti-Sox1 antibodies. The nuclei were stained with TO-PRO-3. Wnt3a treatment decreased Otx1-positive cells (*K*) and induced Hoxc8-positive cells (*Q*), whereas the levels of Nestin and Sox1 expression were not significantly affected. Otx1- or Hoxc8-positive cells also expressed Sox1, suggesting that these cells are neural progenitors.

Immunostaining of Cultured Cells. Cultured cells were fixed with 4% paraformaldehyde. Dilution of antibodies was as follows: mAb to Nestin (Pharmingen), 1:500; polyclonal antibody (pAb) to Sox1 (sex-determining region Y box 1; provided by R. Lovell-Badge, National Institute for Medical Research, London; ref. 25), 1:500; mAb to Otx1 (orthodenticle homolog 1; Developmental Studies Hybridoma Bank, University of Iowa, Iowa City), 1:1; mAb to Hoxc8 (homeobox C8; Covance, Princeton), 1:100. Secondary antibodies were rhodamine red- or FITC-conjugated (ICN). The cells were photographed with a Carl Zeiss LSM510 laser scanning microscope.

Results and Discussion

We generated a null mutation in the ICAT gene by means of homologous recombination in ES cells (Fig. 1*A*). Of 300 recombinant clones screened by PCR, we identified three clones that showed site-specific recombination. Two of the three clones gave rise to chimeras that transmitted the mutated allele to their offspring. We confirmed correct recombination by PCR and Southern blot analysis (Fig. 1 *B* and *C*), and loss of ICAT protein expression was observed by immunoblotting analysis (Fig. 1*D*). ICAT$^{-/-}$ embryos generated from the two clones exhibited identical phenotypes.

ICAT-heterozygous mice exhibited an apparently normal morphologic appearance and were fertile. Genotypic analysis of embryos from embryonic day 7.5 (E7.5) to E18.5 showed no deviation from the expected Mendelian ratio. However, ICAT$^{-/-}$ embryos showed multiple developmental defects, consistent with our observation that ICAT is expressed ubiquitously in postimplantaion embryos (data not shown).

At E18.5, 51% (35/69) of ICAT$^{-/-}$ embryos exhibited a truncation of the rostral head (Fig. 2 *A* and *C*). Development of the cerebrum was defective in 47% (7/15) of ICAT$^{-/-}$ embryos (Fig. 2*E*). The most severely affected embryos displayed exencephaly and lacked eyes, nose, maxillary bone, and rostral skull [14% (8/57)] (Fig. 2 *A–D* and *F*). These phenotypes resemble those of embryos lacking Dickkopf1 or Six3, negative regulators of Wnt signaling, and are consistent with the notion that repression of Wnt signaling is crucial for forebrain development (13, 17–19). In addition, ≈40% (6/15) of ICAT$^{-/-}$ embryos exhibited a cleft secondary palate (Fig. 2*F*). Consistent with the abnormalities observed in bones

derived from the cephalic neural crest, terminal deoxynucleotidyltransferase-mediated dUTP nick end labeling (TUNEL) staining of the ventral craniofacial mesenchyme, the first branchial arch, revealed an increase in apoptotic cell number in ICAT$^{-/-}$ embryos compared with control embryos at E11.0 (Fig. 2 *G* and *H*). Intriguingly, these phenotypes are similar to those observed in mutant mice possessing a specific disruption in the *APC* (adenomatous polyposis coli) gene in neural crest cell (26). This finding suggests that Wnt signaling is aberrantly activated in neural crest-derived cells in ICAT$^{-/-}$ embryos, inducing their apoptosis and leading to craniofacial defects. Additionally, ICAT$^{-/-}$ mice suffered a rupture of the gut and died within several hours after birth [99% (194/196)] (Fig. 2*I*). This rupture might be caused by the degeneration of the enteric nervous system, which is derived from neural crest cells. Furthermore, 13% (4/32) of ICAT$^{-/-}$ embryos lacked kidneys but possessed adrenal glands (Fig. 2 *J* and *K*), suggesting that ICAT plays an important role in the development of the kidneys through the regulation of β-catenin signaling.

To investigate the forebrain phenotype at earlier stages, we analyzed the expression of a number of markers. We found that anterior neural plate expression of Six3 and brain factor 1 (BF-1) was barely detectable in ICAT$^{-/-}$ embryos (Fig. 3 *A* and *C*). In E8.0 wild-type embryos, Irx3 (Iroquois homeobox protein 3) was expressed in the posterior neural plate, complementarily to Six3 expression in the anterior. In ICAT$^{-/-}$ embryos, however, Irx3 was also expressed in the anterior neural plate (Fig. 3*B*). In contrast to this marked alteration in the expression of anterior–posterior markers, expression of neural progenitor markers, such as Nestin and Sox1, and the neuronal marker class III β-tubulin was similar between wild-type and ICAT$^{-/-}$ embryos at E8.5 (Fig. 3*D–F*). These results suggest that general neural induction occurs normally but that neural fate is posteriorized in ICAT$^{-/-}$ embryos.

It is known that ES cells can be efficiently differentiated into neurons by a stromal cell-derived inducing activity (SDIA), which accumulates on the surface of PA6 stromal cells. Furthermore, it has been reported that SDIA induces the generation of neural progenitor cells from ES cells in a time course similar to that observed *in vivo* (22). We therefore used ES cells cocultured with PA6 cells to analyze directly the function of ICAT and Wnt signaling in the determination of cell fate in the nervous system. Because ES cell lines are derived from the inner cell mass of blastocyst-stage embryos at E4.0 and the anterior–posterior patterning of the epiblast is in progress at E6.0 *in vivo* (27), we stimulated SDIA-treated ES cells with Wnt3a after day 2, with the idea that this would correspond to E6.0 *in vivo*. Wnt3a treatment did not significantly affect expression levels of Nestin and Sox1 (Fig. 4). However, Wnt3a treatment suppressed the forebrain markers Six3, BF-1, Emx2 (empty spiracles homolog 2), Otx1, and Otx2 (orthodenticle homolog 2) and induced the hindbrain markers Gbx2 (gastrulation brain homeobox 2) and Hoxb1 (homeobox B1) and the spinal cord markers Irx3, Hoxb4 (homeobox B4), and Hoxc8 (homeobox C8) (Fig. 4).

We next examined the effect of ICAT on the fate of SDIA-treated ES cells. SDIA-treated ES cells were transfected with control vector or ICAT on day 2 and then cultured in the presence of graded concentrations of Wnt3a and 1 μg/ml puromycin during days 3 and 4. Wnt3a suppressed the anterior characteristics and induced posterior characteristics of the cells in a dose-dependent manner (Fig. 5*A*). However, the effects of Wnt3a were suppressed in ICAT-expressing cells, although ICAT did not show any effect on Nestin or Sox1 expression. To investigate the function of endogenous ICAT, we isolated ICAT$^{-/-}$ ES cell lines by culturing ICAT$^{+/-}$ TT2 ES cells, which had transmitted the mutated allele through the germ line in medium containing 4 mg/ml G418. ICAT$^{+/-}$ clones that survived under the same conditions were used as a control. Each cell line was cultured on PA6 and induced to differentiate into neurons. We found that levels of Nestin and Sox1 expression in SDIA-treated ICAT$^{-/-}$ ES cell lines were comparable to those in the SDIA-treated control ES cell lines, but neural fate was posteriorized in SDIA-treated ICAT$^{-/-}$ ES cells, as indicated by the induction of hindbrain and spinal cord markers and repression of forebrain markers (Fig. 5*B*). These results suggest that ICAT induces forebrain cells by inhibiting Wnt signaling in differentiating ES cells.

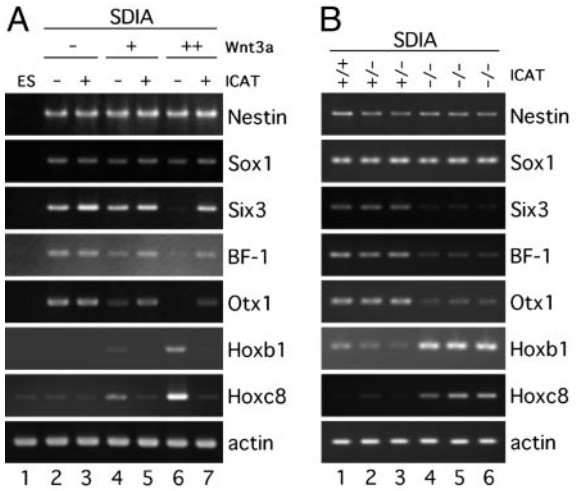

Fig. 5. ICAT induces forebrain cells by inhibiting Wnt signaling in differentiating ES cells. (*A*) Semiquantitative RT-PCR analysis of ICAT-transfected MG1.19 ES cells. Lane 1, undifferentiated ES cells. Lanes 2–7, SDIA-treated ES cells transfected with control vector (lanes 2, 4, and 6) or ICAT (lanes 3, 5, and 7) on day 2 and then cultured in the presence of graded concentrations of Wnt3a (lanes 2 and 3, 0 ng/ml; lane 4 and 5, 10 ng/ml; lane 6 and 7, 30 ng/ml) and 1 μg/ml puromycin during days 3 and 4. Total RNA was isolated on day 6. Wnt3a suppressed the anterior character and induced a posterior character in a dose-dependent manner (lanes 2, 4, and 6). The effects of Wnt3a were inhibited by ICAT. The day on which ES cells were seeded on PA6 was designated day 0. (*B*) Semiquantitative RT-PCR analysis of parental TT2 ES cells (+/+), two heterozygous clones (+/−), and three homozygous clones (−/−). Each cell line was cultured on PA6 cells for 6 days. General neural induction occurred normally, but neural fate was posteriorized in SDIA-treated ICAT$^{-/-}$ ES cells.

Our results suggest that ICAT plays an important role in the anteriorization of neural cells by inhibiting the posteriorizing activity of Wnt signaling. It is believed that brain formation in the mouse embryo requires two organizers, the anterior visceral endoderm and the node and its derivatives (27). However, by using SDIA-treated ES cells, which differentiate with high efficiency into neural progenitors under defined conditions, we demonstrated that ICAT/Wnt signaling could directly change the fate of neural progenitor cells along the anterior–posterior axis in the absence of organizers. Although it has recently been reported that Wnt signaling plays a crucial role in the self-renewal of stem cells (28–33), our results revealed that Wnt signaling exerts different functions depending on the particular state of the stem cells. Our findings could provide a new approach to cell replacement therapy for neurological disorders.

We thank Y. Kanai, T. Sato, and M. Uchikawa for their comments; H. Niwa for pCAG-IP vector; R. Lovell-Badge for pAb to Sox1; and the Developmental Studies Hybridoma Bank for mAb to Otx1. This work was supported by Grants-in-Aid for Scientific Research on Priority Areas and the Organization for Pharmaceutical Safety and Research.

1. Miller, J. R. & Moon, R. T. (1996) *Genes Dev.* **10,** 2527–2539.
2. Cadigan, K. M. & Nusse, R. (1997) *Genes Dev.* **11,** 3286–3305.
3. Eastman, Q. & Grosschedl, R. (1999) *Curr. Opin. Cell Biol.* **11,** 233–240.
4. Peifer, M. & Polakis, P. (2000) *Science* **287,** 1606–1609.
5. Huelsken, J. & Birchmeier, W. (2001) *Curr. Opin. Genet. Dev.* **11,** 547–553.
6. Stark, K., Vainio, S., Vassileva, G. & McMahon, A. P. (1994) *Nature* **372,** 679–683.
7. Aubert, J., Dunstan, H., Chambers, I. & Smith, A. (2002) *Nat. Biotechnol.* **20,** 1208–1210.
8. Kielman, M. F., Rindapaa, M., Gaspar, C., van Poppel, N., Breukel, C., van Leeuwen, S., Taketo, M. M., Roberts, S., Smits, R. & Fodde, R. (2002) *Nat. Genet.* **32,** 594–605.
9. Tago, K., Nakamura, T., Nishita, M., Hyodo, J., Nagai, S., Murata, Y., Adachi, S., Ohwada, S., Morishita, Y., Shibuya, H., *et al.* (2000) *Genes Dev.* **14,** 1741–1749.
10. Sekiya, T., Nakamura, T., Kazuki, Y., Oshimura, M., Kohu, K., Tago, K., Ohwada, S. & Akiyama, T. (2002) *Cancer Res.* **62,** 3322–3326.
11. Graham, T. A., Clements, W. K., Kimelman, D. & Xu, W. (2002) *Mol. Cell* **10,** 563–571 (2002).
12. Daniels, D. L. & Weis, W. I. (2002) *Mol. Cell* **10,** 573–584.
13. McGrew, L. L., Hoppler, S. & Moon, R. T. (1997) *Mech. Dev.* **69,** 105–114.
14. Niehrs, C. (1999) *Trends Genet.* **15,** 314–319.
15. Kiecker, C. & Niehrs, C. (2001) *Development (London)* **128,** 4189–4201.
16. Nordström, U., Jessell, T. M. & Edlund, T. (2002) *Nat. Neurosci.* **5,** 525–532.
17. Mukhopadhyay, M., Shtrom, S., Rodriguez-Esteban, C., Chen, L., Tsukui, T., Gomer, L., Dorward, D. W., Glinka, A., Grinberg, A., Huang, S.-P., *et al.* (2001) *Dev. Cell* **1,** 423–434.
18. Lagutin, O. V., Zhu, C. C., Kobayashi, D., Topczewski, J., Shimamura, K., Puelles, L., Russell, H. R., McKinnon, P. J., Solnica-Krezel, L., Oliver, G., *et al.* (2003) *Genes Dev.* **17,** 368–379.
19. Kim, C.-H., Oda, T., Itoh, M., Jiang, D., Artinger, K. B., Chandrasekharappa, S. C., Driever, W. & Chitnis, A. B. (2000) *Nature* **407,** 913–916.
20. Heisenberg, C. P., Houart, C., Take-Uchi, M., Rauch, G. J., Young, N., Coutinho, P., Masai, I., Caneparo, L., Concha, M. L., Geisler, R., *et al.* (2001) *Genes Dev.* **15,** 1427–1434.
21. van de Water, S., van de Wetering, M., Joore, J., Esseling, J., Bink, R., Clevers, H. & Zivkovic, D. (2001) *Development (London)* **128,** 3877–3888.
22. Kawasaki, H., Mizuseki, K., Nishikawa, S., Kaneko, S., Kuwana, Y., Nakanishi, S., Nishikawa, S.-I. & Sasai, Y. (2000) *Neuron* **28,** 31–40.
23. Shibamoto, S., Higano, K., Takada, R., Ito, F., Takeichi, M. & Takada, S. (1998) *Genes Cells* **3,** 659–670.
24. Niwa, H., Masui, S., Chambers, I., Smith, A. G. & Miyazaki, J. (2002) *Mol. Cell. Biol.* **22,** 1526–1536.
25. Pevny, L. H., Sockanathan, S., Placzek, M. & Lovell-Badge, R. (1998) *Development (London)* **125,** 1967–1978.
26. Hasegawa, S., Sato, T., Akazawa, H., Okada, H., Maeno, A., Ito, M., Sugitani, Y., Shibata, H., Miyazaki, J., Katsuki, M., *et al.* (2001) *Proc. Natl. Acad. Sci. USA* **99,** 297–302.
27. Beddington, R. S. P. & Robertson, E. J. (1999) *Cell* **96,** 195–209.
28. Ikeya, M., Lee, S. M., Johnson, J. E., McMahon, A. P. & Takada, S. (1997) *Nature* **389,** 966–970.
29. Korinek, V., Barker, N., Moerer, P., van Donselaar, E., Huls, G., Peters, P. J. & Clevers, H. (1998) *Nat. Genet.* **19,** 379–383.
30. Chenn, A. & Walsh, C. A. (2002) *Science* **297,** 365–369.
31. Reya, T., Duncan, A. W., Ailles, L., Domen, J., Scherer, D. C., Willert, K., Hintz, L., Nusse, R. & Weissman, I. L. (2003) *Nature* **423,** 409–414.
32. Willert, K., Brown, J. D., Danenberg, E., Duncan, A. W., Weissman, I. L., Reya, T., Yates, J. R., III, & Nusse, R. (2003) *Nature* **423,** 448–452.
33. Sato, N., Meijer, L., Skaltsounis, L., Greengard, P. & Brivanlou, A. H. (2004) *Nat. Med.* **10,** 55–63.